Simulation Study on Application of Nonlinear Model Predictive Control to the Superfluid Helium Cryogenic Circuit ⋆

Rafal Noga [*,**] **Toshiyuki Ohtsuka** [***] **Cesar de Prada** [**]
Enrique Blanco [*] **Juan Casas** [*]

[*] *European Organization for Nuclear Research, CERN CH-1211, Genève 23, Switzerland*
[**] *University of Valladolid, c/ Real de Burgos s/n., 47011 Valladolid, Spain*
[***] *Osaka University, 1-3 Machikaneyama, Toyonaka, Osaka 560-8531, Japan (e-mail: mail@rafal-noga.com).*

Abstract: In the 27 km circumference Large Hadron Collider, the temperature of more than 1600 main superconducting magnets is stabilized below 2 K by the Superfluid Helium Cryogenic Circuit. The key component of the circuit's Standard Cell is an over 100 m long bayonet heat exchanger with two phase flow of superfluid helium, He II, that is integrated into the magnets submerged in a static bath of He II. The magnets operate under constraints, at variable conditions and their temperature dynamics is highly nonlinear, exhibiting variable dead times of response. We present a simulation study on the application of Nonlinear Model Predictive Control for the temperature stabilization. The controller is based on a simplified, first principles model of the circuit and C/GMRES online optimization algorithm. The good performance with small computational cost of the C/GMRES and real-time feasibility of NMPC are highlighted.

Keywords: nonlinear control, model-based control, predictive control, cryogenic temperatures

1. INTRODUCTION

The Large Hadron Collider (LHC) at the European Organization for Nuclear Research (CERN) is the world's highest energy particle accelerator and collider. In the 27 km circumference LHC, more than 1600 NbTi superconducting magnets produce the very strong magnetic fields used for guiding and focusing of particles being accelerated (Brüning et al. (2004)). Superfluid phase of helium 4, called He II, is used to cool and thermally stabilize the high performance magnets operated at temperatures below 2 K, enabling their very compact design. Cryogenic circuits using He II can be found in other large scale projects using superconducting magnets (Tavian (2000)).

1.1 Superfluid Helium Cryogenic Circuit

The Superfluid Helium Cryogenic Circuit (SHCC), also known as the 1.9 K Cooling Loop, is used to cool down and stabilize the temperature of the LHC main superconducting magnets. It was developed at CERN based on the novel concept of He II bayonet heat exchanger (BHX)(Lebrun et al. (1997)). In each 106.9 m long Standard Cell (SC) of the SHCC, one BHX is integrated into eight magnets and

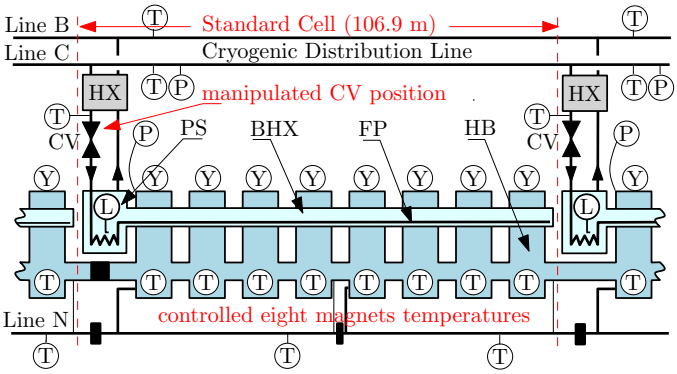

Fig. 1. Standard Cell of the Superfluid Helium Cryogenic Circuit at the LHC. The key circuit components are: bayonet heat exchanger (BHX), helium bath (HB), feeding pipe (FP), control valve (CV), subcooling heat exchanger (HX) and phase separator (PS). The instrumentation consists of thermometers (T), electric heaters (Y), pressure (P) and level (L) sensors.

the assembly is submerged in a common, static, pressurized He II Bath (HB), see Fig. 1. The over 100 m long BHX with inner two phase flow of saturated helium at very low pressure (VLP) can be regarded as quasi-isothermal heat sink and provides cooling to the magnets. The cooling power is proportional to helium mass flow rate that is controlled by a control valve (CV). A Phase Separator (PS) is located at the BHX outlet in order to accumulate helium in case of BHX overflow, to assure pure vapor flow

⋆ Part of this work was done during the stay of the first author at Osaka University for the "FrontierLab@OsakaU" programme. This work was supported by Spanish Government (project DPI2009-12805), University of Valladolid, CERN, Osaka University, Japan Student Services Organization and Grant-in-Aid for Scientific Research (C) No. 21560465

into the VLP Line B of the Cryogenic Distribution Line (QRL). Every two or three neighboring SCs, which are hydraulically connected (share a common HB), compose a Sub-Sector of the SHCC. 27 SCs are distributed over each of the eight, 3.3 km long sectors of the LHC (Gubello et al. (2006)). Helium is supplied to the SCs from a compressor station located at the sector extremity via the QRL.

The nominal operational magnet temperature is 1.9 K and the maximal temperature is constrained because the thermal conductivity of He II in the HB [1] peaks at $T = 1.94$ K and vanishes at lambda (phase) transition temperature $T_\lambda \approx 2.17$ K (CRYODATA INC. (1999), Srinivasan and Hofmann (1985)). Other constraints are associated with maximal He II level in the PS, the CV capacity and the sum of coolant mass flow rates over 27 SCs in a sector and its rate of change.

The dynamics between the CV position, the single manipulated variable used [2], and the controlled, and the measured, magnet temperatures exhibit strong nonlinearities. These are mainly related to: equal percentage CV characteristics, counter-flow heat transfer in He II, BHX cooling power distribution and physical properties of He II (heat capacity and superfluid heat conductivity). The significant SC length causes dead time of response, which varies strongly due to the presence of the nonlinearities. Moreover, SCs in a Sub-Sector are very strongly thermally coupled through heat flows in He II.

1.2 PI and LQ control for the SHCC

Currently the maximal temperature of LHC superconducting magnets is stablized separately over each SC using a Proportional Integral (PI) controller. Due to the nonlinearities and the variable dead times of response, the PI must be tuned in a conservative manner in order to obtain satisfactory performance at various setpoints and heat loads magnitudes. In order to assure enough evaporation rate in the BHX to avoid overflow, the optimal setpoint $T_{sp,0}$ is adjusted with respect to the saturation temperature measured at the compressor station $T_{s,CCS}$ keeping minimum temperature margin $\Delta T_{sp} = 0.08$ K

$$T_{sp} = \max(T_{sp,0}, T_{s,CCS} + \Delta T_{sp}). \quad (1)$$

The margin corresponds to the worst case pressure drop between the compressor station and a SC. Its relatively high value reduces the safety margin to the maximal temperature in case of degradation of VLP.

The PI control performance has been simulated using the first principles, distributed parameter model of the SHCC, see Fig. 2. In the simulation, the PI is tuned more aggressively than in the LHC and system input linearization has been applied to compensate for the equal-percentage characteristics of the CV. A smaller value $\Delta T_{sp} = 0.020$ K has been successfully used assuming that the saturation temperature at a particular SC $T_{s,SC}$ is known. The performance changes considerably as a function of the heat loads q_l and the $T_{s,SC}$. At the low $T_{s,SC}$, during first 7 h of the simulation, the closed loop dynamics of maximal magnets temperature in each SC are

[1] at pressure $p = 1.3$ bar

[2] The electric heaters installed in most of the magnets are not intended to be used for temperature stabilization

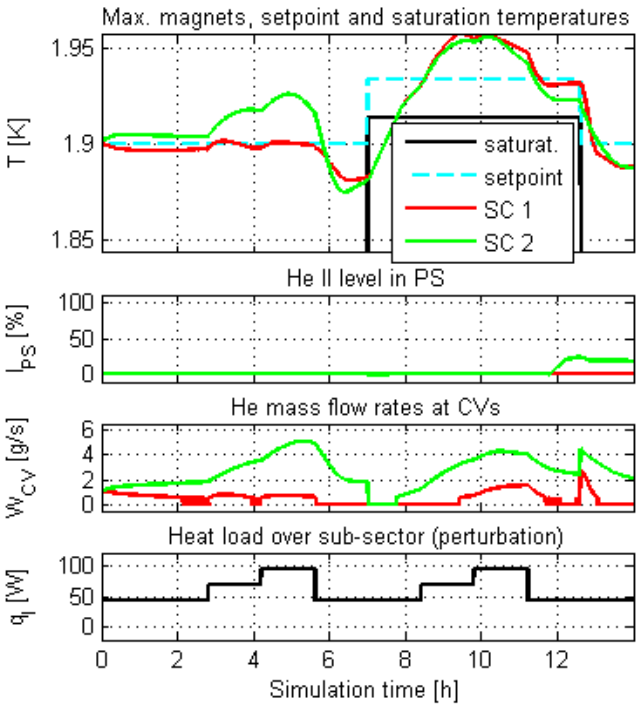

Fig. 2. Simulated performance of the PI controller.

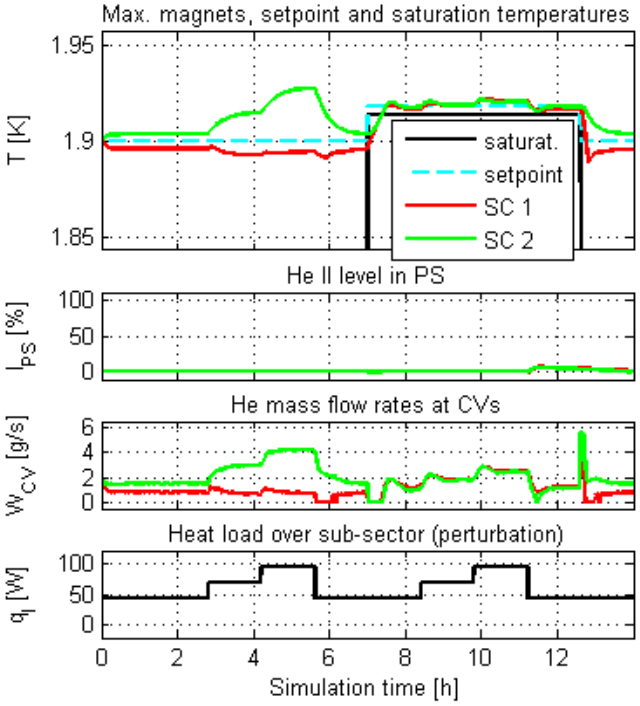

Fig. 3. Simulated performance of the LQ controller.

different due to the thermal coupling that drives one of the CV coolant mass flow rates W_{CV} close to zero and thus, the corresponding BHX is not used. This effect is observed during LHC operation. The control performance is slightly better as the saturation temperature approaches the magnet temperatures.

The performance of Linear Quadratic (LQ) control applied to the SHCC has been simulated, see Fig. 3. The controller gain has been calculated based on a simplified version

of the SHCC model, linearized at $T_{s,SC} = 1.895$ K, corresponding to $\Delta T_{sp} = 0.005$ K that is much smaller than used in the PI. If $T_{s,SC} > 1.895$ K, the steady state HB temperature distribution is shifted in order to keep the ΔT_{sp}. The LQ performance is excellent at high $T_{s,SC}$ and is strongly degraded at lower values due to the coupling and varying steady state temperature distribution.

1.3 Model Predictive Control for the SHCC

Flaemster (2000) has developed a first principles model of the lumped magnet temperature dynamics at the 42.5 m long String 1 with distributed He II mass in the BHX. Then, linear Model Predictive Controllers (MPC) have been developed for versions of the SHCC used in the LHC prototypes String 1 and String 2 (Flaemster (2000); Blanco (2001); Gomes et al. (2004)). Also, a simplified, first principles model of lumped magnets temperature dynamics with non-distributed He II mass in the BHX has been developed for the 30 m long Inner Triplet Heat Exchanger Test Unit (IT-HXTU). Based on the simplified model, Nonlinear MPC (NMPC) for the SHCC at the IT-HXTU has been developed and successfully commissioned. In the NMPC, Sequential Quadratic Programming (SQP) has been applied to minimize a cost function, evaluated via simulation of the model (Blanco et al. (2009)). This NMPC was then applied to the SHCC at the 106.9 m long full scale LHC prototype String 2 Phase 3 showing a non acceptable degraded performance due to the dynamics of this circuit that was different from that at the IT-HXTU.

Subsequently, first principles, distributed parameter, models of the magnets temperature dynamics at the full scale prototype (Noga (2007); Noga and de Prada (2008)) and at the LHC (Noga et al. (2010)) have been developed. Based on the simplified version of the model and Continuation/Generalized Minimum Residual (C/GMRES) algorithm, application of NMPC to the Sub-Sector of the SHCC at the LHC has been studied. The NMPC has the potential to cope with the nonlinear system dynamics and the couplings between SCs respecting constraints related to the PS overflow, the maximal magnet temperature and the CV capacity. Real time feasibility of a simplified NMPC setup has been shown (Noga et al. (2010)).

In this paper, the simulation study on the application of NMPC to the LHC magnets temperature stabilization in a wide range of BHX saturation temperatures, based on the BHX overflow prediction, is presented. This section introduced the SHCC and the motivation for the NMPC development. Next, the simplified model and the C/GMRES algorithm are briefly reviewed. Then, setup of the NMPC is described and its performance is compared against that of PI controller with plant input linearization. Finally, the small computational cost of C/GMRES method and resulting real-time feasibility are highlighted.

2. SIMPLIFIED SHCC MODEL

The simplified model is used in the online optimization of the control action for the NMPC. It is a first principles, distributed parameter model, optimized for low computational cost by:

- capturing a small number of the most significant aspects of the nonlinear process dynamics,
- extensively using approximations of continuous and smooth functions that allow the explicit evaluation of Jacobians needed during the optimization,
- using helium mass flow into the BHX as model input (instead of CV position), and the BHX helium overflow as output (instead of PS He level),
- reducing the number of spatial discretization steps to five per SC

The model is valid at HB temperatures below T_λ. The temperature dynamics of the superconducting magnets is equivalent to that of the HB. It is calculated based on an energy conservation principle applied to the HB, which in 1D is a single PDE. By spatial discretization using finite volume approach, the PDE is transformed into a set of ODEs describing the average temperature dynamics in each of N_x finite volumes

$$\frac{\mathrm{d}T_{m,i}(t)}{\mathrm{d}t} = c_v^{-1}\left(T_{m,i}\right)\ \frac{L}{M}\ \frac{\Delta q_i(t)}{\Delta x}, \quad i = 1...N_x, \qquad (2)$$

where L, M correspond to the length and mass of SC and $\Delta x = L/N_x$ is the discretization interval. The inverse of He II specific heat capacity is approximated as $c_v^{-1}(T_m) = 10^{-4}\ \left(6.22\ dT_m^2 - 7.257\ dT_m + 2.556\right)$, with $dT_m = T_m - 1.9$ K. The heat balance over a finite volume i

$$\Delta q_i(t) = \Delta q_{l,i} - \Delta q_{c,i} - \Delta q_{h,i} \qquad (3)$$

involves sums of heat loads $\Delta q_{l,i}$ and cooling power $\Delta q_{c,i}$ over the interval $(i-1)\ \Delta x < x < i\ \Delta x$ and the difference between heat transfers in the He II at its extremities $\Delta q_{h,i} = q_{h,i+1/2} - q_{h,i-1/2}$.

The total heat load into the HB q_l is a perturbation to the system assumed to be equally distributed, thus

$$\Delta q_{l,i} = q_l \frac{\Delta x}{L}. \qquad (4)$$

The heat transfer in the superfluid is highly nonlinear as $\mathrm{d}T/\mathrm{d}x = f(q_s^3)$. This nonlinearity introduces stiffness in the set of ODEs, which must be limited by using the modified formula (Noga et al. (2010))

$$q_{h,i+1/2} = -A_m\ F^{\frac{1}{3}}(T_{m,i+1/2})\ \Delta T_{m,i+1/2}/\Delta x \times \left(\left(2\ \Delta_{\mathrm{d}T_m/\mathrm{d}x}\right)^2 + \left(\Delta T_{m,i+1/2}/\Delta x\right)^2\right)^{-\frac{1}{3}} \qquad (5)$$

in order to enable fast time integration. The coefficient $\Delta_{\mathrm{d}T_m/\mathrm{d}x}$ controls the tradeoff between the fastest mode time constant and the approximation error. The estimated cross-section area for heat transfer in the HB $A_m = 0.0123$ m2. The superfluid thermal conductivity function $F(T)$ is approximated around its maximum as $F^{1/3} = 2.5 \times 10^4$. In the finite volume scheme, the temperature gradient $\Delta T_{m,i+1/2}/\Delta x = (T_{m,i+1} - T_{m,i})/\Delta x$, and the temperature at the finite volume extremity $T_{m,i+1/2} = (T_{m,i} + T_{m,i+1})/2$. If the extremity corresponds to that of a HB equipped with a plug, the heat transfer $q_{s,i+1/2} = 0$.

The BHX is discretized in the same manner as the HB. The BHX cooling power density over a finite volume is a function of temperatures of magnets and saturation of He II in the BHX T_s, BHX inclination $\mathrm{d}y/\mathrm{d}x$ and He II mass flow rate in the BHX $W_{s,i-1/2}$:

$$\frac{\mathrm{d}q_{c,i}}{\mathrm{d}x}(x) = \begin{cases} 94.89\,(T_{m,i} - T_s)\ (\mathrm{d}y/\mathrm{d}x)^{-0.103} \\ \times W_{s,i-1/2}^{0.1803}\ T_s^3 \quad \text{if } T_{m,i} > T_s \\ 0 \quad \text{otherwise.} \end{cases} \tag{6}$$

The saturation temperature $T_s = T_{s,SC}$ is a model input, corresponding to a non-measured perturbation. Another input is the manipulated He II mass flow rate at the BHX inlet $W_s(0)$.

The cooling power over a control volume is calculated respecting the fact that He II mass flow rate in the BHX can be only non-negative:

$$\Delta q_{c,i} = (W_{s,i-1/2} - W_{s,i+1/2})\ \Delta_H, \tag{7}$$

with $W_{s,i+1/2} = \max(0,\ W_{s,i-1/2} - (\mathrm{d}q_{c,i}/\mathrm{d}x)\ \Delta x/\Delta_H)$. $\Delta_H = 23.4\ 10^3$ J/kg is the He latent heat of evaporation.

The non-negative function and that in Eq. (6) are not smooth. In order to enable explicit Jacobian calculation in the NMPC, the smooth approximation is used

$$\max(x, 0) \approx f(x) := 0.5\left(x + \left(x^2 + 4\ a^2\right)^{\frac{1}{2}} - x^{\frac{1}{2}}\right) \tag{8}$$

with parameter a to control the tradeoff between precision and the maximal value of $\mathrm{d}f/\mathrm{d}x$.

3. NMPC USING C/GMRES METHOD

The control engineering notation is used in this section: $x(t) \in \mathbb{R}^n$ is the state vector and $u(t) \in \mathbb{R}^{m_u}$ is the input vector of a general nonlinear system.

In NMPC, also known as Receding Horizon Control (RHC), an open loop optimal control problem is solved over the future time horizon taken from the current time t to T ahead:

$$\text{minimize } J = \phi(x(t+T)) + \int_t^{t+T} L(x(t'), u(t'))\ \mathrm{d}t', \tag{9}$$

subject to equality constraints

$$\dot{x} = f(x(t), u(t)),\ C(x(t), u(t)) = 0 \tag{10}$$

corresponding to system dynamics and an arbitrary m_c dimensional vector-valued function, respectively. Inequality constraints are transformed to equality constraints by introducing dummy variables. Current state $x(t)$ is known. The problem is reformulated using Lagrange multipliers $\lambda(t)$ and $\mu(t)$ as

$$\text{minimize } \bar{J} = \phi + \int_t^{t+T} L + \lambda^T\ (f - \dot{x}) + \mu^T\ C\ \mathrm{d}t'. \tag{11}$$

Feedback control is realized by applying only the initial part of the optimized input trajectory and continuously repeating the optimization using current measurements and receding the time horizon as the time passes.

3.1 Necessary optimality condition

In order to perform the minimization numerically, $u(t)$ and $\mu(t)$ are parameterized using N discrete inputs $u_i^*(t)$ and Lagrange multipliers $\mu_i^*(t)$

$$u(t) = \sum_{i=0}^{N-1} \sigma_i(t)\ u_i^*(t),\ \mu(t) = \sum_{i=0}^{N-1} \sigma_i(t)\ \mu_i^*(t) \tag{12}$$

with basis window functions:

$$\sigma_i(t) = \begin{cases} 1 & \text{if } t_i \le t' < t_{i+1} \\ 0 & \text{otherwise.} \end{cases} \tag{13}$$

The continuous approach with parametrization (Noga et al. (2010)) allows separation of control horizon discretization grid $t_i,\ i = 1..N$ from the length of the state/costate integration step. This is crucial in case of stiff systems that need a very short integration step. In contrast, they both coincide in a discrete approach (Ohtsuka (2004)).

The necessary condition for an extremum of $\bar{J}$ are: the constraints (10), the costate dynamics

$$\dot{\lambda} = -H_x^T(x, u, \lambda, \mu),\ \lambda(t+T) = \phi_x^T(x(t+T)), \tag{14}$$

with Hamiltonian $H = L + \lambda^T f + \mu^T C$, and a $(m_u + m_c)\,N$ dimensional nonlinear equation (Bryson and Ho (1975); Ohtsuka (2004); Noga et al. (2010)),

$$F(U(t), x(t), t) = 0, \tag{15}$$

$$F := [H_{u,0}\ C_0^T\ \cdots\ H_{u,N-1}\ C_{N-1}^T]^T, \tag{16}$$

$$U(t) := [u_0^{*T}\ \mu_0^{*T}\ \cdots\ u_{N-1}^{*T}\ \mu_{N-1}^{*T}]^T, \tag{17}$$

$$H_{u,i} := \int_{t_i}^{t_{i+1}} H_u\ \mathrm{d}t',\ C_i := \int_{t_i}^{t_{i+1}} C\ \mathrm{d}t'. \tag{18}$$

For a given sequence of $u_i^*(t)$ and $\mu_i^*(t)$, $\dot{x}$ is integrated over the finite horizon $t < t' < t + T$, starting from $x(t)$. Then $\dot{\lambda}$ is integrated backwards from $t + T$ back to t. Finally, $H_{u,i}$ and C_i are evaluated and assembled into the residuum of the necessary optimality condition F.

3.2 C/GMRES method

The C/GMRES algorithm (Ohtsuka (2004)) exploits the fact that the nonlinear equation $F(U(t), x(t), t) = 0$ is solved continuously and its solution, the optimal input trajectory $U(t)$, is expected to change slowly over time as the state of the controlled system evolves and the control horizon moves. C/GMRES traces the time-varying solution without any iterative searches. Note that F is identically zero if the following conditions hold:

$$\mathrm{d}F(U(t), x(t), t)/\mathrm{d}t = -\zeta\ F(U(t), x(t), t), \tag{19}$$

$$F(U(0), x(0), 0) = 0, \tag{20}$$

where ζ is a positive constant to stabilize $F = 0$ against numerical errors and unmodeled disturbances. The condition is rewritten as linear equation for $\dot{U}(t)$

$$F_U\ \dot{U} = -F_x\ \dot{x} - F_t - \zeta\ F \tag{21}$$

that is solved efficiently by a linear solver GMRES (Kelley (1995)) using matrix-vector multiplications. The multiplication $F_U\ \dot{U}$ is approximated using finite differences, thus skipping explicit calculation of the Jacobian F_U. Finally, the solution $U(t)$ is traced by integrating $\dot{U}(t)$.

3.3 Optimal control setup

The goal of the control action is to stabilize the maximal magnet temperature over the assembly of two interconnected SCs, at prescribed level $\max\ x(t) = x_{sp}$. This objective is addressed using an asymmetric quadratic cost

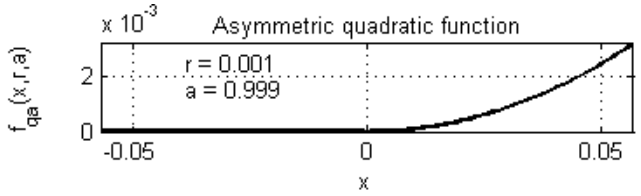

Fig. 4. Asymmetric cost function.

function that penalizes positive deviation from the setpoint much stronger then negative one:

$$f_{qa}((x)_i, r, a) = \frac{[((x)_i^2 + r^2)^{\frac{1}{2}} + a(x)_i]^2 - 2\ a\ r(x)_i - r^2}{(1+a)^2}, \tag{22}$$

for each element $(x)_i$ with tuning parameters r and a, see Fig. 4. Moreover, quadratic weights are assigned to the manipulated variables $u(t)$ and the BHX overflow mass flow rates $W_s(L)$. In order to obtain a well posed optimization problem, a linear weight is put on the dummy input $u_d(t)$ (Seguchi and Ohtsuka (2003)). Thus, the performance index:

$$\begin{aligned}
&\phi = 0 \\
&L = 0.2 \sum_{i=1}^{10} f_{qa}\left((x)_i - x_{sp}, 0.001, 0.999\right) \\
&\quad + 10 \sum_{i=1}^{2} (u_i - u_0)^T\ (u_i - u_0) - 2\ 10^{-4} \sum_{i=1}^{2} u_{d,i} \\
&\quad + 10^3 \sum_{i=1}^{2} W_{s,i}(L)^T\ W_{s,i}(L).
\end{aligned} \tag{23}$$

The setpoint x_{sp} is the same for interconnected cells. The steady state helium flow $u_0 = q_{l,SC,est}/\Delta_H$, with the estimated heat load per SC $q_{l,SC,est}$. Pre-multiplying the performance index by a constant has a strong influence on the C/GMRES performance. Apparently, this scaling provides preconditioning to the linear equation (21).

In the study we directly address only the constraint on CV capacity: $0 < u(t) < u_{max}$ with the maximal mass flow rate $u_{max} = 5$ g/s smaller than the actual valve capacity in order to limit perturbations to the compressors. This inequality constraint is transformed to equality with a dummy input variable u_d:

$$(2\ u - u_{max})^2 + u_d^2 - u_{max}^2 = 0. \tag{24}$$

The maximum PS He level constraint is addressed indirectly by minimizing the BHX overflow. The maximum HB temperature constraint is far from typical operational conditions, thus has been neglected.

3.4 NMPC simulation

The NMPC controller is implemented as a simulation independent C function based on the AutoGenU: An Automatic Code Generation System for Nonlinear Receding Horizon Control (Ohtsuka (2000)). The simplified, analytical model is written in Mathematica® and all derivatives are automatically calculated using symbolic mathematics and saved as C code. The model is discretized using 10 points. As a consequence, 10 states and co-states are integrated over the control horizon with a time step $\Delta t_{max,o} =$ 5.54 s calculated as limit for Euler method convergence, based on eigenvalue analysis of the HB dynamics.

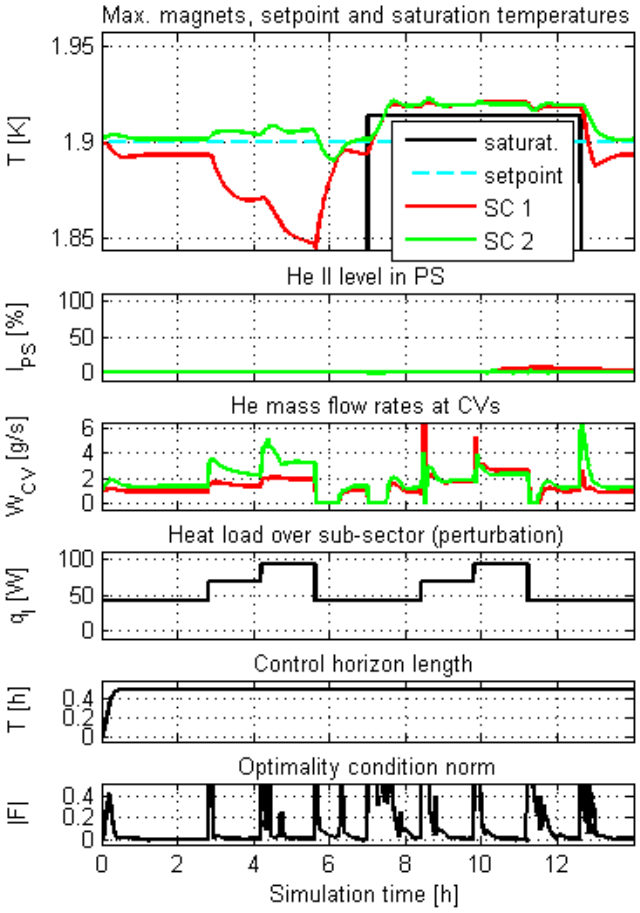

Fig. 5. Simulated performance of the NMPC controller.

The simulation is implemented in MATLAB® . The link to the C code of the controller is established through MEX files. A full, precise model of two interconnected SCs is used to represent the plant. This full model includes the dynamics of He II accumulation in the BHX, uses higher discretization number of 25 points per SC and allows simulation of heat load perturbation effects.

The C/GMRES tracks the optimal trajectory, which must be initialized at the start of the simulation. The initial trajectory is optimized over a reduced number of parameters, using constant inputs trajectory over shortened control horizon length $T_{min}(t) = 0$. After the initialization, the control horizon is subdivided into $N = 10$ intervals, and its length is gradually increased over the simulation to its final value $\lim_{t\to\infty} T(t) = 30$ min, see the subplot $T(t)$ in Fig. 5. The control input is recalculated every 30 seconds of simulated time. This time interval is a crucial C/GMRES parameter, being the integration time step of the input trajectory, it influences the dynamics of the residuum of the optimality condition F. Moreover it has an impact on the disturbance rejection capability.

The NMPC performance is simulated in the presence of varying heat loads on the HB and saturation temperature at the BHX outlet (a function of pressure), see Fig. 5. These are unmeasured perturbations and need to be estimated. However, in the simulation, the values are

supplied directly to the controller, skipping the estimation. At low saturation temperature in the BHX, during first 7 h of the simulation, the NMPC decreases the steady state maximal temperature of one cell as the heat load increases. This compensation of the changing temperature gradient in the other cell reduces the heat transfer between the SCs and is a key to equal distribution of coolant mass flow rates between SCs. In contrast, the PI controller stabilizes the maximal temperature of each SC at the same level, resulting in strong heat transfer between them and vanishing coolant mass flow rate in one of the cells, see Fig. 2. Comparing to previous study (Noga et al. (2010)), the maximal positive temperature offset has been significantly reduced by the introduction of the steady state input u_0 into the performance index. As the saturation temperature is increased suddenly to exceed the setpoint in the second part of the simulation, initially it exceeds the magnet temperatures and no cooling power is available, thus helium introduced in the BHX would first accumulate in the BHX and then in the PS. The reaction of the NMPC is instantaneous and correct: both valves are closed until the magnet temperature rises to a level above the saturation. Then the NMPC stabilizes the temperature at the minimal possible level, adjusted to changing heat loads, without provoking BHX overflow. The steady state maximal magnet temperature is significantly lower than in the case of PI control and similar to that of LQ, where the overflow is avoided by adjusting the setpoint using the fixed safety margin calculated based on worst case scenario. During the whole simulation the residuum of the optimality condition quickly converges back to zero after perturbations are introduced.

The important feature of the C/GMRES method is low computational cost. The optimization problem with with two constraints ($m_c = 2$), two inputs and two dummy inputs ($m_u = 4$), has $N(m_u + m_c) = 10(4 + 2) = 60$ free variables and is solved in less than 0.6 s on a personal computer with 2.4 GHz CPU. Given that the optimization is repeated every 30 seconds, this is $30/0.6 = 50$ times smaller than time available for calculation, enabling further extensions of the NMPC.

4. CONCLUSIONS

NMPC has been designed to stabilize the maximal temperature of LHC superconducting magnets over two interconnected SCs. The controller has been implemented based on the AutoGenU, with derivatives calculated using symbolic mathematics. In simulation, at saturation temperatures much lower than the magnets temperatures, the NMPC stabilizes the maximal temperature of each SC's at different levels enabling equal distribution of cooling power between them. At this conditions, the NMPC performance is superior to that of PI and LQ controllers. At higher saturation temperatures, the NMPC performance is comparable with that of LQ. At this conditions, both controllers are able to stabilize the magnet temperatures much closer to the saturation temperature then the PI, respecting the PS overflow constraint.

Very low computational cost of C/GMRES makes the real time application feasible and enables NMPC extension to whole LHC sector under constraints imposed by the compressor unit. Other possible further developments include: development of state and perturbations estimation and consideration of valve finite rangeability. The controller has been integrated into the LHC cryogenics control system in a test mode and experimental validation is ongoing.

REFERENCES

E Blanco. *Nonlinear Model-based Predictive Control Applied To Large Scale Cryogenics Facilities*. PhD thesis, University of Valladolid, 2001.

E Blanco, C de Prada, S Cristea, and J Casas. Nonlinear predictive control in the LHC accelerator. *Control Eng. Pract.*, 17(10):1136 – 1147, 2009.

OS Brüning, P Collier, P Lebrun, S Myers, R Ostojic, J Poole, and P Proudlock. *LHC Design Report*. CERN, 2004.

A E Bryson and Y Ho. *Applied optimal control : optimization, estimation, and control*. Hemisphere Pub. Corp., 1975.

CRYODATA INC. Hepak v3.4 (computer program), 1999.

B Flaemster. *Investigation, Modelling and Control of the 1.9 K Cooling Loop for Superconducting Magnets for the Large Hadron Collider*. PhD thesis, Trondheim TU, 2000.

P Gomes, C Balle, E Blanco-Viñuela, J Casas-Cubillos, S Pelletier, M A Rodrguez, L Serio, A Suraci, and N Vauthier. Experience with the String2 Cryogenic Instrumentation and Control System. LHC Project Report, 2004.

G Gubello, L Serio, and M Soubiran. The circuits of the LHC Cryogenic System. Engineering Specification, 2006.

C T Kelley. *Iterative Methods for Linear and Nonlinear Equations*. SIAM, 1995.

P Lebrun, L Serio, L Tavian, and R Van Weelderen. Cooling Strings of Superconducting Devices below 2 K: the Helium II Bayonet Heat Exchanger. *Adv. Cryog. Eng., A*, 43A:419 426, 1997.

R Noga. Modeling and control of the String2 LHC Prototype at CERN. Master's thesis, Gdansk University of Technology, University of Karlsruhe, Grenoble Institute of Technology, 2007.

R Noga and C de Prada. First principles modeling of the Large Hadron Collider's (LHC) Super Fluid Helium Cryogenic Circuit. In *Proceedings of 20th European Modeling and Simulation Symposium (EMSS08)*, 2008.

R Noga, T Ohtsuka, C de Prada, E Blanco, and J Casas. Nonlinear Model Predictive Control for the Superfluid Helium Cryogenic Circuit of the Large Hadron Collider. In *Proceedings of the 2010 IEEE International Conference on Control Applications*, pages 1654 – 1659, 2010.

T Ohtsuka. AutoGenU: Readme.txt, 2000. URL `http://www-sc.sys.es.osaka-u.ac.jp/~ohtsuka/`.

T Ohtsuka. A continuation/GMRES method for fast computation of nonlinear receding horizon control. *Automatica*, 40(4):563 – 574, 2004.

H Seguchi and T Ohtsuka. Nonlinear receding horizon control of an underactuated hovercraft. *Internat. J. Robust Nonlinear Control*, 13(3-4):381 – 398, 2003.

R Srinivasan and A Hofmann. Investigations on cooling with forced flow of He II. Part 2. *Cryogenics*, 25(11): 652 – 657, 1985.

L Tavian. Large Cryogenics Systems at 1.8 K. LHC Project Report, 2000.